Metallophysics and Advanced Technologies
Металофіз. новітні технол.
Metallofiz. Noveishie Tekhnol.
2019, vol. 41, No. 9, pp. 1187–1203
https://doi.org/10.15407/mfint.41.09.1187
Reprints available directly from the publisher

CRYSTAL-LATTICE DEFECTS

PACS numbers: 61.50.Lt, 61.72.jj, 61.72.Mm, 61.72.S-, 71.15.Pd, 71.20.-b

Molecular Dynamics Study of the Hydrogen and Carbon Effect on Mobility of Grain Boundaries in α-Iron

S. M. Teus and V. G. Gavriljuk

G. V. Kurdyumov Institute for Metal Physics, N.A.S. of Ukraine,
36 Academician Vernadsky Blvd.,
UA-03142 Kyiv, Ukraine

The effect of hydrogen and carbon on the mobility of a grain boundary in the α-iron is studied by means of molecular dynamics. The calculations are performed within the linear elasticity approach. Both hydrogen and carbon atoms reveal a strong tendency to grain boundary segregation. As shown, the hydrogen atoms, located in the vicinity of the grain boundaries, decrease the activation enthalpy of grain boundary migration, which results in their higher mobility in comparison with the hydrogen-free case. In contrast, the carbon atoms strongly pin the grain boundary at its initial position within the whole range of temperatures and also under the strain used in the modelling. The obtained results are interpreted based on the opposite effect of the studied interstitial elements on the atomic interactions: the increase in the concentration of free electrons due to hydrogen and its decrease due to carbon. As supposed, the hydrogen-caused increase of grain boundaries mobility can be a reason for the early start of recrystallization, as it is observed in the hydrogen-charged iron-based alloys.

Key words: hydrogen, carbon, interatomic bonding, electron structure, grain boundary mobility, molecular dynamics.

Вплив водню та вуглецю на рухливість меж зерен в α-залізі було досліджено із використанням методу молекулярної динаміки. Розрахунки було виконано в рамках пружного наближення. Водень та вуглець виявляють сильну схильність до зерномежової сегрегації. Показано, що знаходячись в околі меж зерен водень знижує значення ентальпії активації їх міграції, що проявляться у підвищеній мобільності меж зерен у порів-

Corresponding author: Sergiy Myronovych Teus
E-mail: teus@imp.kiev.ua

Citation: S. M. Teus and V. G. Gavriljuk, Molecular Dynamics Study of the Hydrogen and Carbon Effect on Mobility of Grain Boundaries in α-Iron, *Metallofiz. Noveishie Tekhnol.*, **41**, No. 9: 1187–1203 (2019), DOI: 10.15407/mfint.41.09.1187.

нянні з випадком ненаводненого зразка. На противагу цьому, атоми вуглецю міцно закріплюють межу зерна на її вихідній позиції на всьому температурному інтервалі і при всіх значеннях деформації, використаних при моделюванні. Отримані результати інтерпретуються базуючись на протилежному впливі елементів на міжатомні взаємодії: підвищення концентрації вільних електронів воднем та їх зниження вуглецем. Припускається, що спричинена воднем підвищена рухливість межі зерна може бути причиною раннього старту рекристалізації, що спостерігається в наводнених сплавах на основі заліза.

Ключові слова: водень, вуглець, міжатомний зв'язок, електронна структура, рухливість межі зерна, молекулярна динаміка.

Влияние водорода и углерода на подвижность границ зёрен в α-железе было исследовано с использованием метода молекулярной динамики. Расчёты выполнены в рамках упругого приближения. Водород и углерод проявляют сильную склонность к зернограничной сегрегации. Показано, что находясь в окрестности границ зёрен, водород понижает значение энтальпии активации их миграции, что проявляется в повышенной мобильности границ зёрен в сравнении с ненаводороженным образцом. В противоположность этому, атомы углерода жёстко закрепляют границу зерна на её первоначальной позиции во всём температурном интервале и при всех значениях деформации, использованных при моделировании. Полученные результаты интерпретируются, основываясь на противоположном влиянии элементов на межатомные взаимодействия: повышении концентрации свободных электронов водородом и их понижении углеродом. Предполагается, что индуцированная водородом повышенная подвижность границы зерна может быть причиной раннего старта рекристаллизации, что наблюдается в наводороженных сплавах на основе железа.

Ключевые слова: водород, углерод, межатомная связь, электронная структура, подвижность границы зерна, молекулярная динамика.

(Received June 2, 2019)

1. INTRODUCTION

It is well known that grain boundaries (GB's) significantly affect mechanical properties of metallic materials. Perhaps Lim and Ray [1] were the first to shed light on the importance of GB structure for their interaction with dislocation slip. Studying the low cycle fatigue in the polycrystalline nickel, they have shown that cavities are formed due to impingement of dislocation slip at grain boundaries. The probability of cavitation increases with the $\sum$ value of the grain boundary. Moreover, the slip-boundary intersection can induce GB migration leading to nucleation and growth of new grains.

The emission of dislocations by GB as a function of their structure

was another effect studied by Lim and Ray [2]. The slip continuity across the GB was found to be higher for the low $\sum$ boundaries in comparison with the high $\sum$ ones.

Earlier, Ponds and Smith [3] proposed a detailed mechanism for absorption of slip dislocations by the high angle GB. The emission or absorption of slip dislocations or blocking of slip by GB has been also in detail studied in [4, 5].

A concept of 'grain boundary design and control' for optimization of mechanical and chemical properties has been introduced by Watanabe [6] claiming that bulk properties can be improved by increasing the number of 'special' grain boundaries close to low Σ orientation relationships. As shown by Shvindlerman and Straumal [7], special grain boundaries exist in a certain range of misorientation angles and the magnitude of this angle range decreases with increasing $\sum$. Following to Watanabe [6] and using a geometric model of crack propagation through the intergranular paths, Aust *et al*. [8] confirmed importance of the $\sum$ grain boundary fraction control in the intergranular corrosion of a Ni-based alloy. While analysing available experimental data on the grain boundary character distribution, one can suppose that GB's with lower energies and low index planes are preferred.

Another approach to characteristics of GB's in the crystals can be based on their excess energy, *i.e.* the difference in the energy between the defected and ideal crystals. As dominant defects in materials, the grain boundaries reveal a wide variation in the excess energy. From this point of view, important is the affinity of interstitial elements to GB's and, correspondingly, the effect of segregation on GB properties, *e.g.* their mobility, which controls recrystallization.

Theoretical methods are widely used to describe the grain boundary interactions with impurity atoms [9–15]. A special attention is paid to GB behaviour under effect of hydrogen and carbon. Both elements have a strong tendency to grain boundary segregation (see *e.g.* [16–18]). Nevertheless, their effect on mechanical properties of materials is completely different.

Hydrogen in the iron-based alloys is known to cause embrittlement, which frequently results in the intergranular fracture [19–21]. By means of molecular static simulation on the iron-hydrogen system [22] it was shown that hydrogen accumulation at the GB causes its decohesion. As for the carbon, using the first-principles calculations, Yamaguchi [11] has shown that the carbon surface segregation energy is smaller than its segregation energy on the grain boundaries. This result is an indication that carbon can increase the GB cohesive energy.

It is worth noting that, in such theoretical studies, the grain boundary is considered as a static defect. The application of external stress could result in GB migration. For example, the shear-coupled grain boundary migration model [23, 24] was proposed to explain the stress-

driven growth of grains at room temperature in the nanocrystalline aluminium [25]. The wide range of materials, where the stress-driven GB migration manifests itself, allows to conclude, that this effect is not restricted to the type of crystal lattice and has a general character. The atmospheres of interstitial atoms around GB usually act as pinning points and, thus, can affect GB mobility under driving force (see, *e.g.*, [26–28]).

The aim of the present research is to perform a comparative study of hydrogen and carbon effect on the grain boundary mobility in the α-iron by means of molecular dynamics.

2. THEORETICAL METHOD

To study mobility of grain boundaries in the α-iron in presence of hydrogen and carbon, the molecular dynamics simulations were carried out using the large-scale atomic/molecular massively parallel simulator (LAMMPS) program package [29]. The simulations were performed on the asymmetric tilt grain boundary Σ5[001](430)/(100) incorporated in the rectangular simulation box with crystallographic orientations <100>, <010> and <001>. The schematic presentation is given in Fig. 1. To construct the grain boundary, the coincidence site lattice theory (CSL) has been used [30, 31], where each half-crystal denoted as 'cell 1' and 'cell 2' is rotated around the tilt axis on different angles and connected together along the obtained GB. To simplify the further strain energy density calculations, the local coordinate system of 'cell 1' coincides with the global axes directions. To satisfy the CSL conditions, dimensions of the global simulation box were $\sim 71 \times 287 \times 30$ Å^3 along the X, Y and Z axes, respectively.

Initial calculations have shown that the variation in the number of atoms in the simulation box does not cause any change in the energy characteristics. The periodic boundary conditions were applied in the X and Z directions of the global coordinate system, whereas the boundaries in Y direction were treated as free surfaces to prevent GB's interaction and allow expansion or contraction in this direction, which depends on the externally applied forces. To obtain the equilibrium structure, the energy minimization procedure was applied to the simulation box amounting to the relaxation of atomic positions and GB internal degrees of freedom.

Initially, the hydrogen atoms were homogeneously distributed within the simulation box taking into account that hydrogen prefers to occupy tetrahedral interstitial positions in the bcc lattice [32, 33]. During subsequent stages of temperature stabilization, the hydrogen and iron atoms are allowed to relax. The bulk hydrogen concentration was equal to 56 wtppm. In contrast to hydrogen, carbon atoms were homogeneously distributed in the area close to the GB. A reason for that is

the much slower diffusion of carbon in comparison to hydrogen and, taking into account the time scales used in the molecular dynamics, a long time should be needed to observe the carbon atoms redistribution. The concentration of carbon atoms in the iron was taken to be of 40 wtppm.

The atomic interactions in the iron-hydrogen system were characterized with potential developed in [34] based on the embedded atom method potential [35–37]. For the Fe–H interaction, an extensive database of energies and atomic configurations obtained by the density functional theory (DFT) calculations was used in order to fit the cross interaction between Fe and H. The pair atomic interactions in the iron–carbon system were approximated with potential developed in [38] with the appropriate description of short-range covalent interactions of carbon *p*-electrons.

At the initial stage, all systems were relaxed using the Gibbs-NPT thermodynamic ensemble, where N is a number of particles, P is a pressure, and T is a temperature. This technique allows to control the internal energy of the system and considers a thermal equilibrium state with a heat bath under fixed temperature. The pressure parameter during the relaxation was controlled using the Parrinello–Rahman

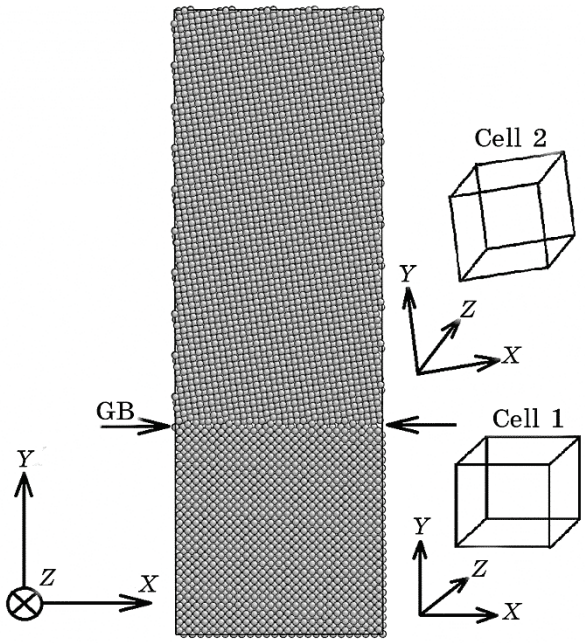

Fig. 1. Schematic representation of simulation box with the asymmetric tilt grain boundary inside.

technique [39]. The Nose–Hoover method [40, 41] was used to keep a constant temperature (T). The pressure was maintained at 0 Pa in all the simulations. To reach and stabilize the parameters, the NPT ensemble has been applied for 1.5 ns.

At the second stage, to initiate the grain boundary migration, a permanent strain has been applied to the simulation box with a components $\varepsilon_x = \varepsilon_z = \varepsilon$ in relation to its global coordinates and the changes in GB position have been observed for the next 4 ns.

3. RESULTS

The asymmetric tilt grain boundary has been chosen because of the method used to initiate GB migration. There are several theoretical methods to study GB mobility [42–49]. In the present research we have chosen the method based on the driving force initiation. Two techniques are widely used for that: (i) to apply the elastic strain to a bi-crystal [42–44] and (ii) to add the artificial energy based on the local orientation of the crystal lattices [45–47]. We used here the first one because of its direct relation to physical processes. Nevertheless, as it has been shown in [50], the simulation results do not depend on the type of applied force under the condition of its linear correlation with GB velocity. An external strain has been applied to the simulation cell with its components along the X and Z directions of the global coordinate system (see Fig. 1). The GB normal strain component, ε_{yy}, was equaled to 0 to prevent the external influence on the grain boundary migration. An additional condition is that, within the elasticity limit, $\varepsilon_{xx} = \varepsilon_{zz} = \varepsilon$ to exclude the appearance of the shear strain and, thus, to avoid the effect of GB sliding on the grain boundary migration.

As it is known and recently confirmed by the experimental study [51], the migration step of the symmetric tilt grain boundaries consists of normal GB migration coupled to the tangential GB shear. On the other hand, as mentioned in [52], sliding does not appear in case of twist and general GB's. By taking into account that, in our case, the collective atomic displacement of the upper cell relative to the lower one is not observed, it is possible to imply that for the studied high-angle asymmetric grain boundary and under above mentioned conditions, the GB sliding is not a necessary crystallographic step in GB migration process. Nevertheless, local tangential atomic displacements in GB plane could not be excluded.

In case of the asymmetric tilt grain boundary and under condition of external strain and bi-crystals elastic anisotropy, the driving force is a result of the energy change across the GB. The energy gradient across the GB appears because of different orientations of 'cell 1' and 'cell 2' in relation to the global coordinate system. Within the linear elastic approach, the strain energy density, U, equals to

$$U = \frac{1}{2}\sigma_{ij}\varepsilon_{ij}, \tag{1}$$

where σ and ε are second rank stress and strain tensors, respectively. Both tensors are related to each other through the generalized Hooke's law:

$$\sigma_{ij} = C_{ijkl}\varepsilon_{kl}, \tag{2}$$

where C_{ijkl} is a fourth rank tensor of elastic constants, with $i, j, k, l = 1$ to 3. By considering the cubic symmetry of cells, the number of independent parameters in the tensor of elastic constants reduces to the three ones: C_{11}, C_{12}, C_{44} (for simplicity, we used Voigt notation here). By combining equations (1) and (2), the driving force of grain boundary migration, P, could be determined as a difference between the strain energy densities of two half-crystals:

$$P = U_{\text{cell2}} - U_{\text{cell1}}. \tag{3}$$

As seen in Fig. 1, the local coordinate system of 'cell 2' is inclined in relation to global coordinates. In such case, the strain tensor for this crystal has to be modified by multiplication on the rotation matrix. The condition of free surfaces allows the simulation box to change its dimension in Y direction without the appearance of stress component along the GB normal, *i.e.* $\sigma_{i3} = 0$, where $i = 1, 2, 3$. The details about strain energy density determination could be found in [42].

A special method has to be developed to determine the grain boundary position in the simulation box with interstitial atoms. A typical approach to get the GB position is to use the Common Neighbour Analysis (CNA) [53, 54]. In case of systems with interstitial atoms, a direct application of such technique does not give satisfactory results. A reason for that can be the following: (i) the bulk concentration of interstitial atoms and their non-homogeneous distribution result in a large number of local distortions of crystal lattice; (ii) rather high simulation temperature and, therefore, large thermal atomic oscillations give too many deviations from the bcc template according to CNA and (iii) local variations in the GB shape and the non-equilibrium hydrogen distribution in the GB plane.

To calculate the grain boundary position, we developed a scheme that is based on a strong affinity of hydrogen (carbon) atoms to GB. The first step was the averaging in the atomic positions before applying the CNA method, which improves the statistics. In the second step, because of the number of broken bonds, the atoms in the GB area are characterized by the increased energy in comparison with the atoms in the bulk. Thus, by performing the screening on the energy per atom value, these atoms could be separated from the others.

At the last stage, the simulation box has been divided into regions parallel to the X axis of global simulation box with the step of approximately 0.3 Å and the number of atoms in each region has been calculated. As a result, the diagram presented in Fig. 2 is constructed, where each bar represents the weight of the average GB position in the current region.

At such consideration, the coordinate of grain boundary has been determined as a mass centre of the diagram:

$$Y_{MC} = \frac{\sum_{i=1}^{N} m_i y_i}{\sum_{i=1}^{N} m_i}, \tag{4}$$

where y is a cell co-ordinate along the Y direction in Fig. 1, m_i is a number of atoms in the i-th cell, N is the total number of regions in the GB.

By means of the mentioned technique, the grain boundary position at each time step has been calculated. In addition, as follows from Fig. 2, the GB width is equal to approximately 8 Å, which is very close to the experimentally determined grain boundary width of ~5 Å [55].

To get a true GB migration under the driving force, it is necessary to be convinced that a variation in internal parameters does not cause the GB movement. Particularly, as shown in [56, 57], the high angle GB Σ29 in copper is quite mobile at elevated temperatures and can migrate without the action of external force.

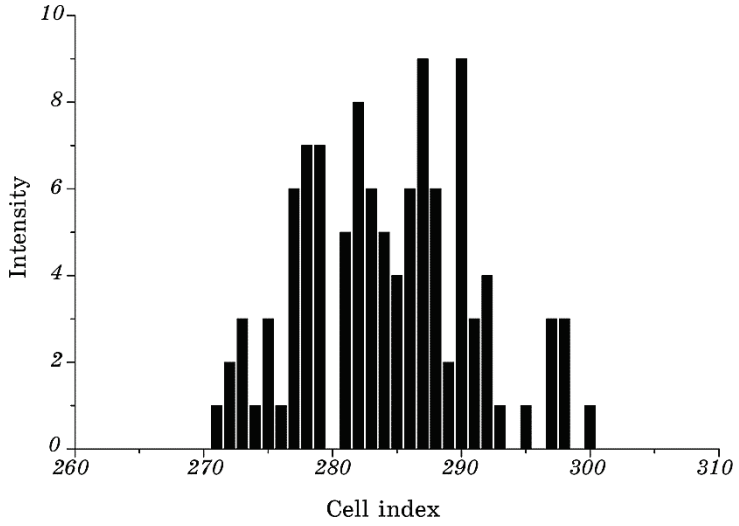

Fig. 2. Diagram to determine the average grain boundary position at a certain step of molecular dynamics.

The effect of temperature on the GB position within time used in the current simulation is shown in Fig. 3. In this Figure and in the following ones, the GB position is represented as a fraction of the simulation box length in direction of GB normal *Y*. It is seen that there is some thermal fluctuation of the grain boundary position with time and the fluctuation amplitude depends on temperature. Nevertheless, its average position could be considered as permanent. In addition, the absence of GB movement under the equilibrium conditions indicates that there is no interaction of GB with free surfaces.

Under tensile strain, the grain boundary is forced to move. The results of simulation of GB migration in the hydrogen-free iron and that doped with 56 wtppm hydrogen are shown in Fig. 4 for different strains at temperature of 1100 K. The change in GB position has been observed during 4 ns.

It has to be mentioned that the temperature used in the simulations exceeds 1000 K. The reasons of such rather high temperature are connected with i) the necessity to observe a GB migration under the action of the driving force and ii) the time scales used in the molecular dynamics calculations. Particularly it means that the conditions have to be applied to the simulation box to observe the whole process of grain boundary migration within the time interval of several nanoseconds. It is worth noting that the temperature in this case affects only the atomic kinetic energy. Also, during the simulations the system is considered as closed in relation to hydrogen escape and hydrogen can only to

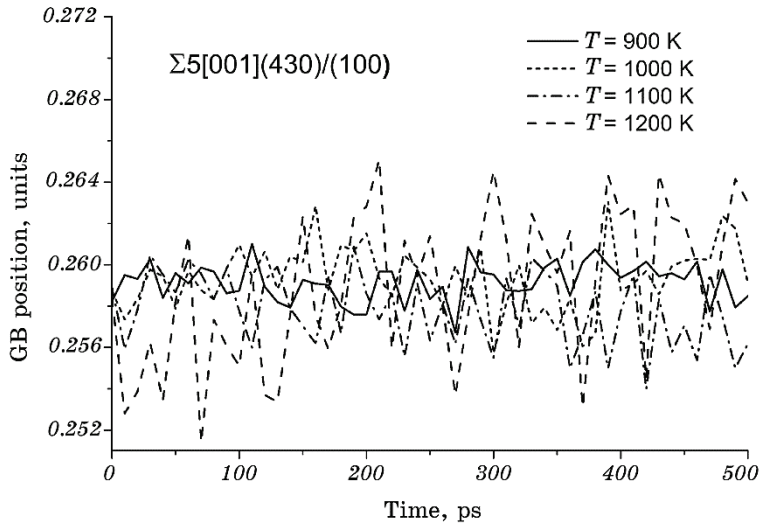

Fig. 3. Variations in grain boundary position in the α-iron with time at different temperatures without the action of external forces.

migrate or to redistribute between the defects of crystal structure. A similar conditions, for example are realized during gaseous hydrogen charging where high temperature and pressure are necessary to keep an increased hydrogen concentration in the material. Thus, during further discussion, the meaning of segregation is the certain amount of hydrogen around the GB that affects its mobility.

All the curves, presented in Fig. 4, reveal a linear behaviour, which corresponds to a steady state grain boundary migration in the iron crystal. With increasing applied strain, the GB moves because of higher driving force. The hydrogen GB segregation leaves unchanged the general linear behaviour. At equal strains, GB migration is higher in the iron crystal doped with hydrogen.

As mentioned above, the determination of grain boundary mobility by means of molecular dynamics simulations is based on the linear elasticity approach. Thus, the range of external deformation applied to the crystal has to be discussed.

In present simulations, the strain level does not exceed 2.5%. It has to be mentioned that this value cannot be very low because, taking into account the time scale of molecular dynamics, it will result in too small distance run by the grain boundary. In addition, atomic oscillations at

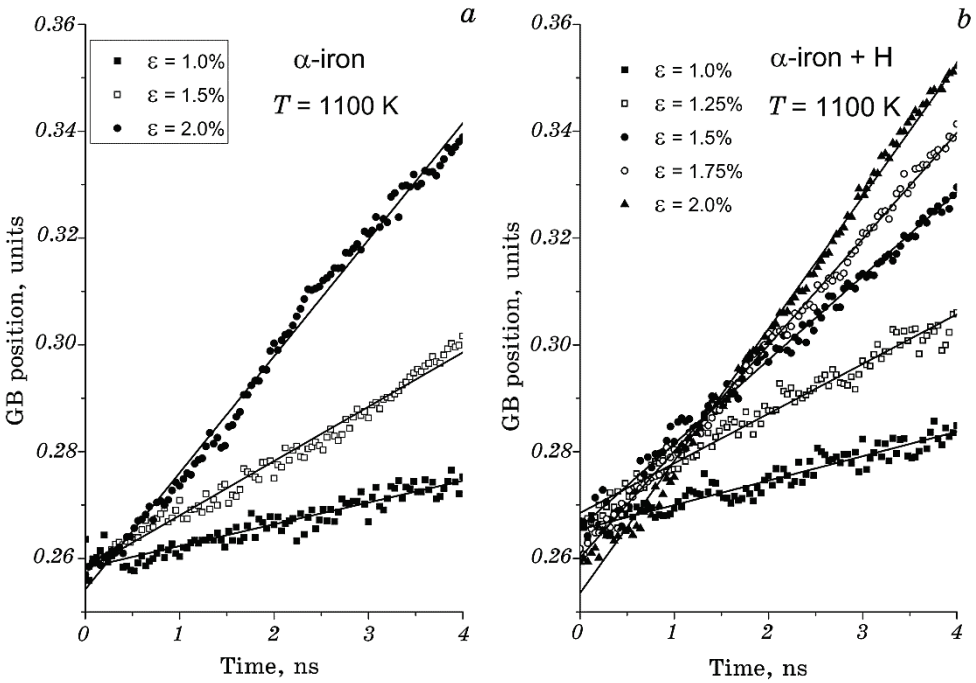

Fig. 4. Change with time of the grain boundary position in the α-iron under different external strains: H-free (*a*); $C_{\text{Hbulk}} = 56$ wtppm (*b*).

elevated temperatures will not provide an appropriate statistics for accurate determination of GB movement. For example, for twist GB migration in aluminium [58], the mobility assessment has been shown to be correct at strains of 4% and temperatures $T > (2/3)T_m$, where T_m is the melting temperature. Zhang *et al.* [42] compared the linear elastic approach with the alternative determination of strain energy density via integration of stress-strain curve for each grain for the asymmetric GB in nickel. It was shown that, at largest strain $\varepsilon = 2\%$, the deviation was approximately 13%. Taking into account the ideal structure of crystals in the simulations and based on the mentioned results, the strain interval used in our modelling is considered to be valid.

The results presented in Fig. 4 allow to find velocity of grain boundary migration under certain strains and temperatures. The variation in the simulation temperature allows to obtain GB velocity as a function of the driving force calculated using equation (3). The results are shown in Fig. 5 for crystals with and without hydrogen.

As follows from the theory of reaction rate, a linear correlation is expected between GB velocity and driving force at its small values [42, 58, 59]. The mobility M of grain boundaries is a temperature activated parameter and its representation in Arrhenius co-ordinates (see inserts in Fig. 5) allows to obtain the activation enthalpy of grain boundary migration ΔH. For the case of the asymmetric tilt grain boundary $\Sigma 5[001](430)/(100)$, we obtained $\Delta H_{\text{H-free}} = 0.99 \pm 0.06$ eV for the hydrogen-free crystal and $\Delta H_{\text{H(56 wtppm)}} = 0.73 \pm 0.03$ eV for that with the bulk hydrogen content of 56 wtppm. It is seen that H segregation at the grain boundaries decreases the activation enthalpy for their movement.

It is worth noting that redistribution of hydrogen atoms takes place in the course of stabilization stage because the grain boundaries and

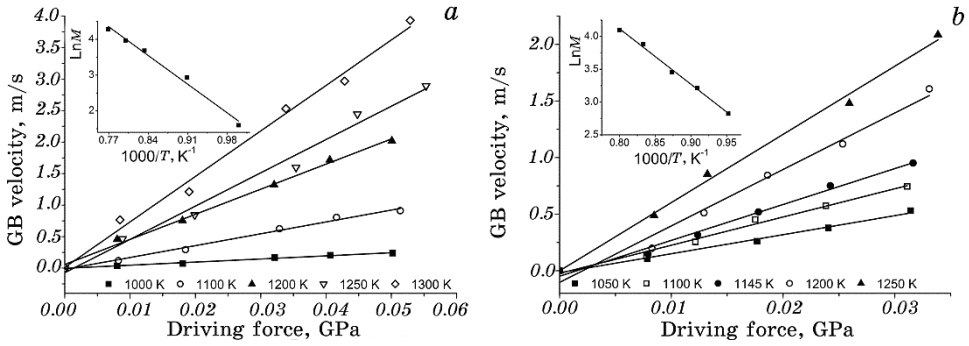

Fig. 5. Grain boundary velocity as a function of driving force at different temperatures for the H-free simulation cell (*a*) and that with C_{Hbulk} of 56 wtppm (*b*). The temperature dependence of GB mobility is shown in the insert in the Arrhenius co-ordinates.

free surfaces in the simulation cell possess the excess energy. As shown in [60] using first-principles atomic calculations, the fracture surface in the iron-hydrogen solid solution is more preferential for hydrogen segregation in comparison with the GB. In order to estimate the actual hydrogen content at the grain boundary during the steps of molecular dynamics, the area around the GB of 0.8 nm in the width has been selected in the present simulation and the number of hydrogen atoms within this area was calculated and averaged. As a result, the segregated hydrogen content at the grain boundary is of 10.5 wtppm, whereas the rest part of hydrogen, 45.5 wtppm, goes to free surfaces.

As mentioned previously, in contrast to hydrogen, the carbon atoms were initially distributed in the GB area because of their very slow diffusion and short time scales used in molecular dynamics simulations. In Fig. 6, the variation of GB position with time is presented under the strain level of 1.25% and temperatures of 1100 K and 1300 K. It is seen that, under such conditions, only thermal oscillations of the grain boundary take place increasing in their amplitude with increasing temperature.

4. DISCUSSION

In our previous research [61], the grain boundary diffusion of carbon and hydrogen has been studied. By means of theoretical and experimental techniques, it was shown that the activation enthalpy of H and C migration in the selected area of grain boundaries is higher in comparison with that in the bulk. In other words, the grain boundaries

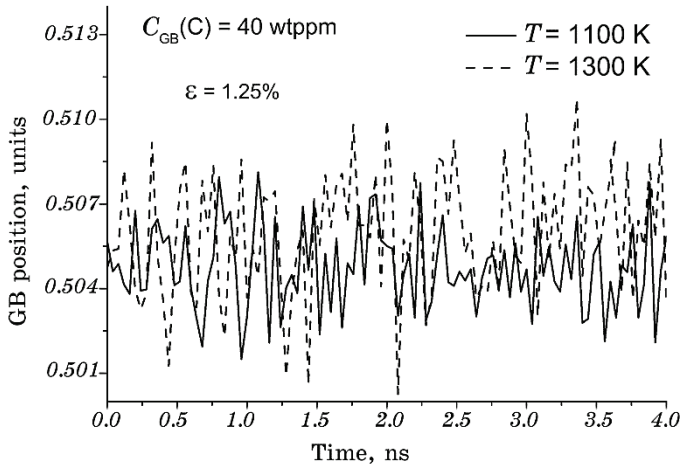

Fig. 6. Variation in grain boundary position with time in the α-iron doped with carbon under strain 1.25% and different temperatures.

substantially decrease the mobility of C and H atoms in their vicinity. This conclusion was derived for the high angle GB's, but it can be extended also to the case of low angle GB's which can be constructed as dislocation arrays.

The presented molecular dynamics simulations of hydrogen effect on the mobility of the asymmetric Σ5[001](430)/(100) tilt grain boundary in the α-iron show that hydrogen decreases the activation enthalpy of GB migration under the action of externally applied strain, *i.e.* increases GB mobility in comparison with the H-free crystal. In contrast, the effect of carbon is opposite.

As follows from the results presented in Fig. 6, only the grain boundary thermal oscillation takes place without any sign of migration at temperatures up to 1300 K and strain of 1.25%. Under such circumstances, the quantitative effect of carbon on the enthalpy of GB migration could not be determined, but it is obvious that its value is higher in comparison with that in the interstitial-free iron. On the other hand, it is quite complicate to compare the theoretically obtained values with the experimental ones. The reasons for that are the following: (i) difficult preparation of bi-crystals with special geometry of grain boundaries and (ii) significant effect on the GB migration caused by the segregation of even small bulk content of impurities, as it was shown, *e.g.*, in [28].

The conclusion about a decrease of recrystallization temperature can be derived from the obtained hydrogen-caused reduction in the activation enthalpy of GB migration. As experimental confirmation of this effect, the results earlier presented in [62] can be referred to. Using the EBSD technique and X-ray diffraction, it was shown that the gaseous hydrogen charging of the previously cold worked 304 austenitic steel at 543 K results in the reverse $\alpha \rightarrow \gamma$ transformation accompanied by the recrystallization. This phenomenon seems to be surprising if to take into account that in the hydrogen-free austenitic steel of 304 type as well as in the more stable 316 steel, the reverse $\alpha \rightarrow \gamma$ transformation occurs at about 823 K independently of the amount of strain-induced α-martensite, see *e.g.* [63], whereas the recrystallization temperature is even much higher, *i.e.* 973 K and 1073 K, respectively.

An alternative interpretation of the hydrogen-caused decrease in the recrystallization temperature can be also based on the hydrogen effect on the concentration of vacancies. It was theoretically predicted [64] and experimentally confirmed [65] that hydrogen in metals increases the thermodynamically equilibrium concentration of vacancies. Taking into account the segregation tendency of hydrogen atoms to the GBs which at the same time are the sinks for vacancies, it is expected that, under driving force, the migration of host atoms constituting grain boundary is accelerated in comparison with the H-free case. However, as follows from the present simulation results, hydro-

gen atoms decrease the activation enthalpy of grain boundary migration and increase its mobility without any excess vacancies. Moreover, the theoretical assessment performed by McLellan [66] shows that carbon atoms also increase the equilibrium concentration of vacancies.

On account of the strong affinity of carbon atoms with the grain boundaries, it is expected that their effect on GB mobility should be similar to that of hydrogen. In contrast, the results of our modelling confirm that carbon atoms pin the GB in its initial position.

This difference in the H and C effect on the grain boundary migration allows us to suppose that a reason for such different behaviour can be searched for in the change of atomic interactions caused by both elements coupled with the mechanism of GB migration.

There are different approaches concerning an atomic mechanism for the grain boundary migration. In a group of models [67, 68], the GB migration is analysed as a thermally activated single- or multi-atomic transport across the boundary. The other approach is based on the transmission electron microscopy studies and relates the GB migration to movement of the grain boundary dislocations which have a component of the step vector out of the GB plane, see *e.g.* [69]. From our point of view, the attention has also to be paid to theoretical results presented in [60]. By means of molecular dynamics, the authors analysed the distribution of planar interatomic bond angles and came to conclusion that GB migration steps consist of local bond rearrangements with formation of domain-like structures and their reordering. If so, the strength of interatomic bonds should play an important role during the rearrangement process and interstitial elements should affect it.

In this relation, it is shown in the ab initio atomic calculations of the electron structure in the hydrogen-containing iron in its f.c.c. [70], as well as in b.c.c. [71] modifications, that hydrogen increases concentration of free electrons and, thereby, enhances the metallic component of interatomic bonding. Depending on the GB migration mechanism, this should ease the reordering processes and atomic jumps across the grain boundary. Under condition of mobile hydrogen atoms, it should result in the accelerated grain boundary migration. The effect of carbon atoms is opposite: the decrease in the conduction electrons concentration promotes the covalent interatomic interactions [72], which strengthens the grain boundary against rearrangement of atomic bonds. Combining with much higher activation enthalpy of carbon diffusion, as compared to that of hydrogen, a significant reduction in GB mobility is expected.

It is also worth noting that the change in atomic interactions caused by interstitial elements has similar consequences for dislocation properties, particularly dislocation mobility. The hydrogen atmospheres around the dislocation locally decrease its specific energy and thus increase the dislocation mobility [70, 72]. Within the framework of elec-

tron delocalization molecular orbital (ASED-MO) theory, it was shown for the b.c.c. iron [73], that carbon atoms create a Fe–C–Fe 'bridge' in the area of $a/2[1\bar{1}1]$ dislocation, which should prevent the dislocation displacement under the shear stress.

5. CONCLUSIONS

1. By means of molecular dynamics simulation of hydrogen effect on mobility of the asymmetric tilt grain boundary, it is shown that, be segregated at the grain boundary, hydrogen decreases the activation enthalpy of the GB migration and, thus, increases its mobility.
2. In contrast to hydrogen, the carbon segregation at the grain boundary causes the opposite effect. Within the range of temperatures, only the grain boundary thermal atomic oscillations take place under external strain, which means that carbon increases the activation enthalpy of GB migration.
3. The proposed interpretation of different H and C effects on the grain boundary mobility is based on the change in the atomic interactions caused by interstitial elements. Hydrogen enhances the metallic component of interatomic bonding, which promotes the bond rearrangement in the GB area or atomic jumps across the GB. In contrast, carbon increases the covalent component of atomic interactions, which strengthens the Fe–C–Fe bonds and lowers GB mobility.

REFERENCES

1. L. C. Lim and R. Raj. *Acta Metal.*, **32**(8): 1183 (1984).
2. L. C. Lim and R. Raj, *Acta Metal.*, **33**(8):1577-1583 (1985).
3. R. C Pond and D. A. Smith, *Philos. Mag.*, **36**(2): 353 (1977).
4. N. Hansen, A, Horsewell T. Leffers, and H. Lilholt, *Proceedings of the 2nd Riso International Symposium on Metallurgy and Materials Science (September 14–18, Riso)* (Denmark, Roskilde: National Laboratory: 1981).
5. T. N. Backer, *Yield, Flow and Fracture of Polycrystals* (London: Applied Science Pub.: 1983).
6. T. Watanabe, *J Phys. Colloques.*, **49**(C5): 507 (1988).
7. L. S. Shvindlerman and B. B. Straumal. *Acta Metall.*, 33(9): 1735 (1985).
8. K. T. Aust, U. Erb, and G. Palumbo. *Mater. Sci. Eng. A*, **176**: 329 (1994).
9. W. T. Geng, A. J. Freeman, R. Wu, and G.B. Olson, *Phys. Rev. B*, **62**: 6208 (2000).
10. J. P. Buban, K. Matsunaga, J. Chen, N. Shibata, W. Y. Ching, T. Yamamoto, and Y. Ikuhara, *Science*, **311**: 212 (2006).
11. M. Yamaguchi, *Metall. Mater. Trans.*, **42**: 319 (2011).
12. D. N. Seidman, B. W. Krakauer, and D. Udler, *J. Phys. Chem. Solids*, **55**(10): 1035 (1994).
13. A. Sutton and R. Balluffi, *Interfaces in Crystalline Materials* (Oxford, UK: Clarendon Press: 1995).

14. E. D. Hondros and M. P. Seah, *Int. Met. Rev.*, **22**: 262 (1977).
15. M. Yamaguchi, M. Shiga, and H. Kaburaki. *Science*, **307**: 393 (2005).
16. J. S. Wang, *Eng. Fract. Mech.*, **68**(6): 647 (2001).
17. T. Ohmisawa, S. Uchiyama, and N. Nagumo, *J. Alloys Compd.*, **356–357**: 290 (2003).
18. Yu. N. Petrov, *Scr. Metall. Mater.*, **29**: 1471 (1993).
19. K. H. Lo, C. H. Shek, and J. K. L. Lai, *Mater. Sci. Eng. R*, **65**: 39 (2009).
20. P. Novak, R. Yuan, B. P. Somerday, P. Sofronis, and R. O. Ritchie, *J. Mech. Phys. Solids*, **58**: 206 (2010).
21. L. Zhong, R. Wu, A. J. Freeman, and G. B. Olson, *Phys. Rev. B*, **62** (21): 13938 (2000).
22. H. Fukushima and H. K. Birnbaum. *Acta Metall.*, **32**(6): 851 (1984).
23. J. W. Cahn and J. E. Taylor, *Acta Mater.*, **52**(14): 4887 (2004).
24. J. W. Cahn, Y. Mishin, and A. Suzuki, *Acta Mater.*, **54** (19): 4953 (2006).
25. T. J. Rupert, D. S. Gianola, Y. Gan, and K. J. Hemker, *Science*, **326**: 1686 (2009).
26. B. B. Straumal, V. G. Sursayeva, and L. S. Shvindlerman, *Phys. Met. Metalloved.*, **49**: 102 (1980).
27. V. Yu. Aristov, Ch. V. Kopetsky, V. G. Sursayeva, and L. S. Shvindlerman, *Reports of USSR Academy of Sciences*, **225** (14): 804 (1975) (in Russian).
28. L. S. Shvindlerman, G. Gottstein, and D. A. Molodov, *phys. status solidi (a)*, **160** (2): 419 (1997).
29. S. Plimpton, *J. Comp. Phys.*, **117** (1): 1 (1995).
30. S. Ranganathan, *Acta Cryst.*, **21**: 197 (1966).
31. M. A. Fortes, *phys. status solidi (b)*, **54** (1): 311 (1972).
32. D. E. Jiang and E. A. Carter, *Phys. Rev B*, **70**: 064102 (2004).
33. J. K. Norskov, *Phys. Rev. B*, **26** (6): 2875 (1982).
34. A. Ramasubramaniam, M. Itakura, and E. Carter, *Phys. Rev. B*, **79** (17): 174101 (2009).
35. M. I. Mendelev, S. Han, D. J. Srolovitz, G. J. Ackland, D. Y. Sun, and M. Asta, *Philos. Mag.*, **83**: 3977 (2003).
36. G. J. Ackland, M. I. Mendelev, D. J. Srolovitz, S. Han, and A. V. Barashev, *J. Phys. Condens. Mat.*, **16** (27): S2629 (2004).
37. M. W. Finnis and J. E. Sinclair, *Philos. Mag A*, **50**: 45 (1984).
38. D. J. Hepburn and G. J. Ackland, *Phys. Rev. B*, **78** (16): 165115 (2008).
39. M. Parrinello and A. Rahman, *J. Appl Phys.*, **52**: 7182 (1981).
40. S. Nose, *Mol. Phys.*, **52**: 255 (1984).
41. W. G. Hoover, *Phys. Rev. A*, **31** (3): 1695 (1985).
42. H. Zhang, M. I. Mendelev, and D. J. Srolovitz, *Acta Mater.*, **52** (9): 2569 (2004).
43. H. Zhang, M. I. Mendelev, and D.J. Srolovitz, *Scr. Mater.*, **52**: 1193 (2005).
44. B. Schonfelder, P. Keblinski, D. Wolf, and S. R. Phillpot, *Mater. Sci. Forum*, **294–296**: 9 (1998).
45. D. L. Olmsted, E. A. Holm, and S. M. Foiles, *Acta Mater.*, **57** (13): 3704 (2009).
46. K. G. F. Janssens, D. Olmsted, E. A. Holm, S. M. Foiles, S. J. Plimpton, and P. M. Derlet, *Nature Mater.*, 5: 124 (2006).
47. D. L. Olmsted, S. M. Foiles, and E. A. Holm, *Scr. Mater.*, **57**: 1161 (2007).
48. Z. T. Trautt, M. Upmanyu, and A. Karma, *Science*, **314**: 632 (2006).
49. S. M. Foiles and J. J. Hoyt, *Acta Mater.*, **54** (12): 3351 (2006).

50. M. I. Mendelev, C. Deng, C. A. Schuh, and D. J. Srolovitz, *Modelling Simul. Mater. Sci. Eng.*, **21**: 045017 (2013).
51. J.-E. Brandenburg and D. A. Molodov, *Scr. Mater.*, **163**: 96 (2019).
52. J. M. Rickman, S. R. Phillpot, D. Wolf, D. L. Woodraska, and S. Yip, *J. Mater. Res.*, **6** (11): 2291 (1991).
53. D. Faken and H. Jonsson, *Comput. Mater. Sci.*, **2** (2): 279 (1994).
54. H. Tsuzuki, P. S. Branicio, and J. P. Rino, *Comput. Phys. Commn.*, **177** (6): 518 (2007).
55. A. Inoue, H. Nitta, and Y. Iijima, *Acta Mater.*, **55** (17): 5910 (2007).
56. J. F. Lutsko, D. Wolf, S. Yip, S. R. Phillpot, and T. Nguyen, *Phys. Rev. B*, **38** (16): 11572 (1988).
57. J. F. Lutsko, D. Wolf, S. R. Phillpot, and S. Yip, *Phys. Rev. B*, **40** (5): 2841 (1989).
58. B. Schonfelder, D. Wolf, S. R. Phillpot, and M. Furtkamp, *Interface Sci.*, **5** (4): 245 (1997).
59. K. Lucke and H.-P. Stuwe, (Ed. L. Himmel) *Recovery and Recrystallization of Metals* (New York: Interscience: 1963), p. 171.
60. M. Yamaguchi, J. Kameda, K.-I. Ebihara, M. Itakura, and H. Kaburaki, *Philos, Mag.*, **92** (11): 1349 (2012).
61. S. M. Teus, V. F. Mazanko, J.-M. Olive, and V. G. Gavriljuk, *Acta Mater.*, **69**: 105 (2014).
62. V. M. Shyvanyuk, Y. Mine, and S. M. Teus, *Scr. Mater.*, **67**: 979 (2012).
63. C. Herrera, C. L. Plaut, and A. F. Padilha, *Mater. Sci. Forum*, **550**: 423 (2007).
64. A. A. Smirnov, *Metal Physics*, **13** (11): 21 (1991) (in Russian).
65. V. G. Gavriljuk, V. N. Bugaev, Yu. N. Petrov, A. V. Tarasenko, and B. Z. Yanchitsky, *Scr. Mater.*, **34** (6): 903 (1996).
66. R. B.McLellan, *J. Phys. Chem. Solids*, **49** (10): 1213 (1988).
67. N. F. Mott, *Proc. Phys. Soc.*, **60**: 391 (1948).
68. D. Turnbull, *Trans AIME*, **191**: 661 (1951).
69. C. M. F. Rae and D. A. Smith, *Philos. Mag. A*, **41** (4): 477 (1980).
70. S. M. Teus, V. N. Shivanyuk, B. D. Shanina, and V. G. Gavriljuk, *phys. status solidi (a)*, **204** (12): 4249 (2007).
71. S. M. Teus and V. G. Gavriljuk, *Materials Lett.*, **258**: 126801 (2020).
72. V. G. Gavriljuk, B. D. Shanina, V. N. Shyvanyuk, and S. M. Teus, *Corros. Rev.*, **31** (2): 33 (2013).
73. S. Simonetti, M. E. Pronsato, G. Brizuela, and A. Juan, *Appl. Surf. Sci.*, **217**: 56 (2003).